Postembryonic development of the posterior lateral line in the zebrafish

Viviana A. Nuñez,[a,b] Andres F. Sarrazin,[a] Nicolas Cubedo,[a] Miguel L. Allende,[b]
Christine Dambly-Chaudière,[a] and Alain Ghysen*,[a]

[a]Laboratory of Neurogenetics, INSERM, Université Montpellier 2, Place Bataillon, Montpellier, France
[b]Center for Genomics of the Cell, Facultad de Ciencias, Universidad de Chile, Casilla 653, Santiago, Chile
*Author for correspondence (email: alain.ghysen@univ-montp2.fr)

SUMMARY The posterior lateral line (PLL) of zebrafish comprises seven to eight sense organs at the end of embryogenesis, arranged in a single antero-posterior line that extends along the horizontal myoseptum from the ear to the tip of the tail. At the end of larval life, four antero-posterior lines extend on the trunk and tail, comprising together around 60 sense organs. The embryonic pattern is largely conserved among teleosts, although adult patterns are very diverse. Here we describe the transition from embryonic to juvenile pattern in the zebrafish, to provide a framework for understanding how the diversity of adult patterns comes about. We show that the four lines that extend over the adult body originate from latent precursors laid down by migrating primordia that arise during embryogenesis. We conclude that, in zebrafish, the entire development of the PLL system up to adulthood can be traced back to events that took place during the first 2 days of life. We also show that the transition from embryonic to adult pattern involves few distinct operations, suggesting that the diversity of patterns among adult teleosts may be due to differential control of these few operations acting upon common embryonic precursors.

INTRODUCTION

Animal morphologies are the outcome of two distinct processes: embryogenesis and postembryonic development (which may comprise larval, juvenile, mature, and senescent phases). The embryonic/postembryonic transition has particular relevance to evolutionary studies because embryonic forms are usually much more conserved than later forms. In fish, the posterior lateral line (PLL) system comprises discrete mechanosensory organs, the neuromasts, arranged in reproducible patterns, which diverge markedly between different species (Webb 1989). The pattern that is formed during embryogenesis is remarkably similar, however, in the zebrafish, a basal species, and in the turbot, a species that belongs to the highly derived flatfish group (Pichon and Ghysen 2004). It seems likely, therefore, that PLL diversity among teleosts is largely generated during postembryonic development.

The transition from embryonic to juvenile PLL has not been studied in any fish so far. In the zebrafish, the embryonic PLL is fully developed at 48 hpf (hours postfertilization). It comprises five neuromasts aligned laterally along the body and tail, and two to three terminal (ter) neuromasts at the tip of the tail. Over the next several weeks the number of neuromasts increases steadily until the juvenile pattern is achieved. The juvenile PLL comprises about 60 neuromasts arranged in four lines: ventral, lateral, dorso-lateral, and dorsal (Ledent 2002). The PLL pattern does not change further except that

each neuromast buds off accessory neuromasts that remain closely packed to form a "stitch." The number of PLL neuromasts keeps extending throughout adult life by this budding process, up to several hundred organs, whereas maintaining the overall pattern of four lines present in the juvenile fish.

In this article we examine the transition from the embryonic to the juvenile pattern in zebrafish, and we describe the different processes that lead from one to the other. We propose that the complexity of the adult pattern directly originates from the simplicity of the embryonic pattern, even though the adult pattern takes weeks or months to complete. We conjecture that the almost infinite interspecific variation of the PLL pattern may depend much more on the modulation of these few processes in time and space, than on the addition of new generative mechanisms.

MATERIALS AND METHODS

Fish care

Zygotes obtained by natural spawning were collected soon after egg laying and were transferred to Petri dishes in 1 mM NaCl tank water. Methylene blue was routinely added as antiseptic (0.5 mg/l final). Embryos were fed with Novotom powder (http:www.jbl.de) from 4 dpf (days postfertilization) on. They were periodically challenged with *Artemia* larvae (obtained from Salins du Midi) and as

soon as they began to feed they were shifted to a diet of ZM100 (http:www.zmsystems.co.uk) or ZM200 at later larval stages, complemented twice a week with *Artemia*.

Fish lines

The *golden* zebrafish, a lightly pigmented line (Lamason et al. 2005) that we used extensively because the dark pigmented stripes of the juvenile make the alkaline phosphatase labeling method unsuitable for neuromast detection, were obtained from Singapore through a local company, Antinea. The *cldnb:gfp* reporter line, which we used because it allows one to visualize interneuromast cells in addition to primordium and neuromasts (Haas and Gilmour 2006), was given by D. Gilmour. Migration of the PLL primordium is slightly delayed in this line (about 1 somite/h, instead of 1.7 in wild-type embryos), and the average number of neuromasts deposited along the myoseptum is closer to seven than to five (6.8, $N = 40$ embryos). The average distance between consecutive neuromasts, starting at L2, is correspondingly reduced from five somites in the wild type to 3.7 in *cldnb:gfp* embryos ($N = 40$), and neuromasts that are two somites or even one somite apart are unusual but not exceptional. The *foxd3:gfp* line marks glial as well as pigment cells (Gilmour et al. 2002), and was mostly used for glial ablation experiments. It was obtained from the Tübingen stock center. In the sqET20 line, GFP is specifically expressed by the mantle cells of the neuromasts, and by the interneuromast cells (Parinov et al. 2004). This line was given by V. Khorz.

Measuring fish development

Ages are expressed as hpf or days postfertilization (dpf). As the larvae grow, however, age becomes an ineffective measure of development because development is highly asynchronous within a given population, and size becomes a better indicator of developmental stage. The "standard length" of a fish is normally measured from the tip of the lower jaw to the posterior end of the hypural bone (Anderson and Gutreuter 1983). In this article we used as standard length the distance between the anterior end of the larva and the caudal end of the notochord, which is a very good approximation of the standard length and somewhat easier to measure.

KAEDE photoconversion

For photoconversion experiments, KAEDE mRNA was transcribed from a template plasmid (obtained from Miguel Concha). The plasmid was digested with *NotI* and mRNA was synthetized with the SP6 RNA polymerase using mMessage mMachine (Ambion). KAEDE mRNA was injected at 165 pg/embryo at the one-to-two cell stage, using an orange filter on the dissection scope. Injected embryos were incubated in complete darkness until the appropriate stage. We selected the brightest embryos using low-intensity blue light on the microscope. These embryos were anesthetized in tricaine, oriented, and mounted in agar 0.5%, all under orange light. Photoconversion (Ando et al. 2002) was carried out with a Zeiss Axioplan microscope equipped with a 25 μm pinhole, using a grid in the eyepiece to aim the ultraviolet (UV) beam at the desired spot as identified under Nomarski optics. The target area was illuminated with UV light using a × 20 objective, during 30–50 sec. After photoconversion we recorded the position of the ac-

tivated cells with a Zeiss AxioImager M1 equipped with a rhodamine filter and a CoolSnap camera. Embryos were maintained in complete darkness up to 4 days after photoconversion.

Laser ablation

For ablation experiments, we used a Micropoint system equipped with a 440-Coumarin cell and mounted on a Axioplan Zeiss microscope equipped with a long distance, water-immersion × 63 objective. Embryos were mounted in 1% agar, 0.3 × PBS, and anesthetized with 0.0007% benzocaine. The laser beam was then focused on each nucleus, and a short train of pulses was applied. The strength of the laser beam was attenuated to a level such that an early effect of irradiation is visible within a few seconds, and marked changes in nuclear morphology appear within a few minutes. About 12 h after ablation, necrotic cells have been removed and no scar can be detected.

Labeling of neuromasts

Neuromasts were visualized either by fluorescence in the *cldnb:gfp* or SqET20 lines, or by alkaline phosphatase labeling in the *golden* line (Villablanca et al. 2006), or by DiAsp incubation (Collazo et al. 1994) at late stages where adult pigmentation prevents visualization of the alkaline phosphatase labeling.

Detection of neuromast polarity

Neuromast appear polarized after alkaline phosphatase labeling, due to the presence of an anisotropic unlabeled region at the center of each neuromast. The shape and orientation of this unlabeled region were quantified under ImageJ software (http://rsb.info.nih.gov/ij/). Briefly, the outline of the region was defined using the "Find Edges" function. The length of the long and short axes, and the angle between long axis and myoseptum, were then determined using the "Measure" function.

RESULTS

From embryonic to juvenile PLL

The embryonic line is formed by a primordium, primI, that originates just posterior to the otic placode and migrates along the horizontal myoseptum all the way to the tip of the tail (Metcalfe 1985). Migration takes place between 20 and 40 hpf (Kimmel et al. 1995). During its journey, a wild-type primordium deposits five groups of cells that form the lateral neuromasts L1–L5 (Fig. 1A). The primordium shifts to a more ventral pathway when approaching the tip of the tail, and eventually fragments in two or three groups that form the terminal neuromasts (ter, Fig. 1B). Each group differentiates as a neuromast over the 6 h that follow deposition, and the embryonic PLL is fully developed at 48 hpf. The interval between consecutive neuromasts varies around seven somites between L1 and L2, and five somites between L2, L3, L4, and L5 (Gompel et al. 2001). Between the neuromasts lies a single row of interneuromast cells, which have also been deposited
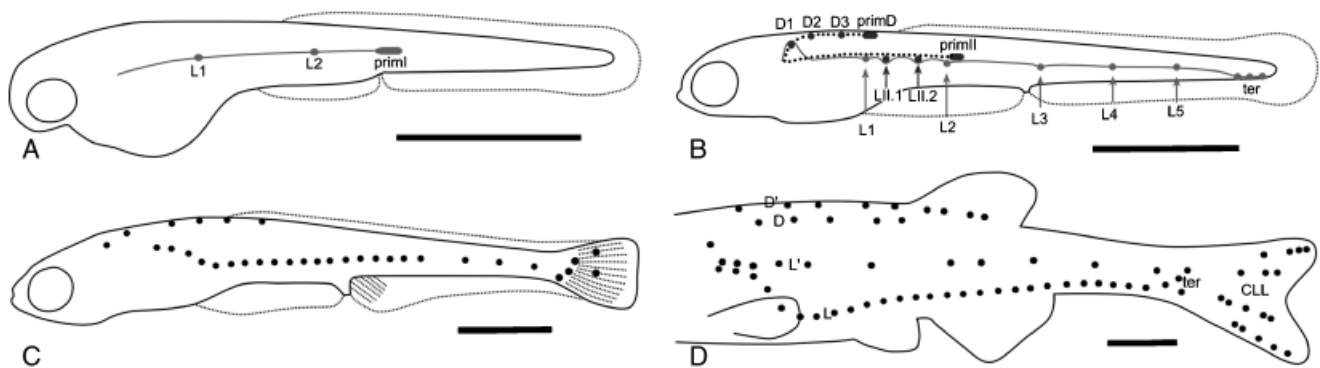
Fig. 1. Major steps of the development of the posterior lateral line pattern in zebrafish. (A) 32 hpf, (B) 48 hpf, and (C) 3–4 weeks. Adapted from Ghysen and Dambly-Chaudière, 2007. D, D′, L, and L′, the four lines of the juvenile PLL system; CLL, caudal fin lateral line. Scale bars: 1 mm.

by the migrating primordium (Fig. 1A, Grant et al. 2005; Lopez-Schier and Hudspeth 2005).

The juvenile pattern is characterized by the presence of four distinct lines (Fig. 1D, Ledent 2002). The ventral-most line comprises about 30 neuromasts; the other three lines comprise fewer neuromasts and occupy, respectively, a lateral, a dorso-lateral, and a dorsal position. The development of the caudal lateral line (CLL) system, which develops on the caudal fin, has been described elsewhere (Dufourcq et al. 2006; Wada et al. 2008). The late larval/juvenile pattern is complete when the larva has reached a standard length of 8 mm, corresponding approximately to 25 days of development. This age is only indicative, because there is considerable variation of size and developmental stage between sibs at this stage, as discussed in "Materials and methods."

Three origins for larval neuromasts

The transition from the embryonic complement of seven to eight neuromasts, to the juvenile pattern of 60 neuromasts, depends on three processes. The first one involves the formation of a new primordium, which splits in two halves around 40 hpf. One-half (primII) follows the same path as primI, whereas the other half (primD) follows a dorsal path, as reported previously (Sapède et al. 2002; Fig. 1B). At 3.5 mm (around 6 dpf), primII has deposited three to four neuromasts, LII.1–LII.4 (Fig. 2A). The neuromasts deposited by primI and primII migrate ventrally, away from the horizontal myoseptum, as soon as they differentiate, except for L1, which remains close to the myoseptum (Fig. 2A–C). The neuromasts deposited by primD also migrate ventrally, albeit to a lower extent. The primII and primD lines extend progressively over the next week and are complete when the larva has reached 5 mm (approximately 2 weeks of development; Fig. 2B, blue arrows, and Table 1).

The second process involved in larval development of the PLL is the formation of intercalary (IC) neuromasts. IC neuromasts form precociously in the absence of glial cells, from the stripe of interneuromast cells deposited by primI, through cell aggregation and proliferation (Grant et al. 2005; Lopez-Schier and Hudspeth 2005). In normal conditions, the formation of IC neuromasts extends over most of larval development (Table 1). The first IC neuromasts appear between L1 and L2, and they progressively fill all intersomitic borders between L1 and L2 that were left vacant by the LII neuromasts (Fig. 2B, red arrows). IC neuromasts continue to develop at more and more posterior positions as larval development proceeds (Figs. 1C and 2C, red arrows). At the end of this second phase, approximately 12 IC neuromasts have formed, and neuromasts of the ventralized line are present at nearly all intersomitic borders between L1 and the tip of the tail (Fig. 2D).

The third and last process of larval PLL development is the formation of two new lines of neuromasts during late larval life (Ledent 2002). One line forms along the horizontal myoseptum, at the position where the L line originally appeared before moving ventrally, and will be called L′. The other line forms along the dorsal midline, at the position where the D line appeared before moving ventrally, and will be called D′ (Fig. 1D). The formation of the L′ and D′ lines extends over late larval life and is complete around the larval–juvenile transition. This transition, which is gradual in the zebrafish, is revealed by a number of morphological changes such as onset of adult pigmentation, development of scales, emergence of the adult pattern of fins and fin rays, etc. We include in Table 1 the formation of scales as one relatively sharp marker of the larval–juvenile transition, at 8.5 mm. Other harbingers of this transition, such as the onset of pelvic fin development or the formation of a lateral band of iridiophores, can be detected earlier, around 6.5 mm.

The PLL pattern is complete at 8 mm, just before the onset of scale formation. Further development of the system is limited to the budding of small clusters of accessory neuromasts (stitches) by each founding neuromast. This process
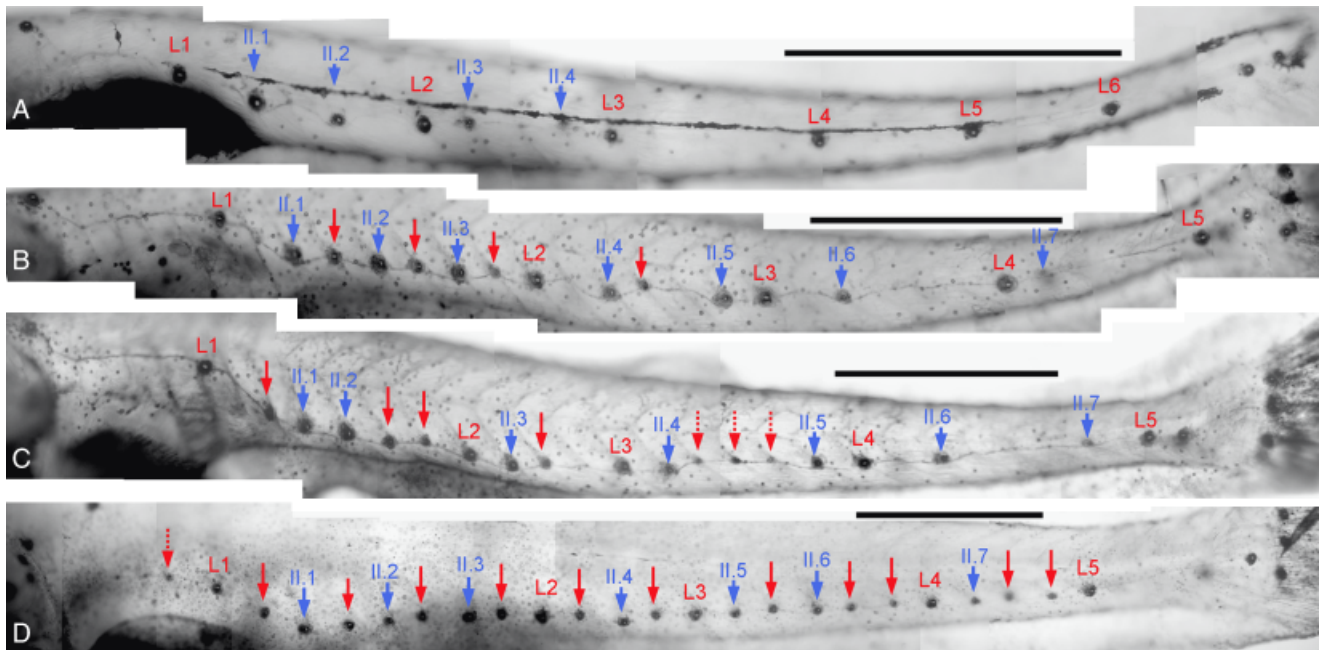
Fig. 2. Larval development of the posterior lateral line. (A) At 3.5 mm (6 dpf), (B) At 5 mm (about 12 days), (C) At 5.5 mm, and (D) At 6.25 mm, the juvenile pattern of one neuromast per somitic border is nearly complete. Blue lettering: primII-derived neuromasts, red arrows: primI-derived IC neuromasts.

Table 1. Summary of PLL larval development

	Size (mm)	3.5	4	4.5	5	5.5	6	6.5	7	7.5	8.0	8.5	9	10
primI- derived	LI	5	=	=	=	=	=	=	=	=	=	=	=	=
	IC		1	2	4	6	9	11	12	=	=	=	=	=
	aIC							2	3	3	=	=	=	=
primII- derived	LII	4	5	6	7	=	=	=	=	=	=	=	=	=
	L′							1	6	10	12	=	=	=
primD- derived	D	3	4	5	6	=	=	=	=	=	=	=	=	=
	D′					2	3	4	5	=	=	=	=	=
	terD						1	2	3	4	=	=	=	=
Other markers	Pits											sp	dp	tp
	Stitches													+
	Scales											±	+	+

The values given are observed in a majority of the embryos; variations are not more than ± 1 for each value. Specifically, among 10 larvae that we examined for each size, the higher limits for the various lines were up to 6 neuromasts for the L line, up to 8 for the LII line, up to 10 (including up to three doublets) for the D line, up to 13 for the L′ line and up to 5 for the anterior intercalary neuromasts (aIC) that develop anterior to L1. Some ambiguity may alter the latter results, for it is not always possible to discriminate with complete certainty the anterior IC neuromasts (aIC) from the anterior-most L′ neuromasts. Symbols =: same as earlier stage; +: present; ±: incipient; sp: shallow supra-orbital pit including the second supra-orbital neuromast, SO2 (Raible and Kruse, 2000); dp: deep supra-orbital pit including SO; tp: three pits form around SO1, SO2 and SO3 and join each other to prefigure the supra-orbital canal (Webb and Shirley 2003).

begins in the early juvenile phase, when the fish has reached 10 mm. In the head, another change takes place after scale formation, at a fish size of about 8.5 mm: the sinking of neuromasts in pits that eventually coalesce to form canals (Table 1).

Phase 1: formation of LII neuromasts

The second primordium, primII, begins to migrate along the horizontal myoseptum around 40 hpf, and reaches L1 at about 48 hpf. primII is smaller than primI and migrates much more slowly (Sapède et al. 2002). The first primII-derived neuromast, LII.1, is laid down at 3 dpf, two somites posterior to L1 on average (Fig. 2A–D). The next three neuromasts, LII.2–LII.4, are deposited over the next 3 days with an average spacing of two somites (Fig. 2).

All hair cells within a neuromast are polarized along the same axis. The axis of hair cell polarity differs, however, between neuromasts deposited by primI and by primII: hair cells of LI neuromasts are polarized along the antero-posterior axis, whereas hair cells of LII neuromasts are polarized along the dorso-ventral axis (Lopez-Schier et al. 2004). Alkaline phosphatase labeling of neuromasts reveals a marked anisotropy, with an unlabeled central region that is clearly elongated (Villablanca et al. 2006, Fig. 3A). We defined the central region as explained in "Materials and methods" (Fig. 3B) and measured its anisotropy as the ratio of its longest versus
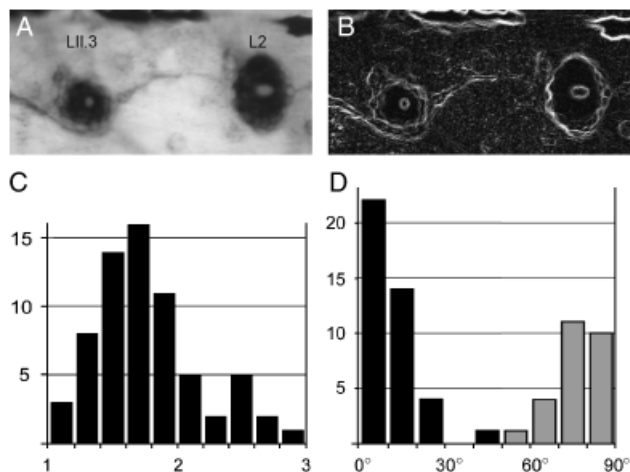
Fig. 3. Neuromast anisotropy. (A) Alkaline phosphatase labeling of PLL in a 5 dpf early larva. (B) Same picture after edge accentuation to facilitate measurement of the longest versus shortest diameter of the central, unlabeled region. (C) Distribution of the ratio between longest and shortest diameters for a sample of 67 neuromasts. (D) Distribution of the angles between the neuromast's long axis and the myoseptum. Black bars: primI-derived neuromasts, gray bars: primII-derived neuromasts.

shortest diameter. The distribution of ratios for the 67 neuromasts of Fig. 2 is shown Fig. 3C. Ratios < 1.5 are typically associated with newly formed neuromasts (e.g., LII.3 in Fig. 3, A and B).

We measured the angles between the long axis and the myoseptum for the same set of 67 neuromasts. We observed that the central unlabeled region tends to be aligned along the antero-posterior axis for the LI neuromasts (Fig. 3D, black bars), and along the dorso-ventral axis for the LII neuromasts (Fig. 3D, gray bars). The difference in long-axis orientation is statistically highly significant ($P < 0.0001$, PAST permutation test, 10,000 replicates, Hammer et al. 2001). The results validate our earlier conclusion that neuromasts display an intrinsic polarity that parallels the structural polarity of the neuromast hair cells, with an antero-posterior orientation for neuromasts derived from primI, and a dorso-ventral orientation for neuromasts derived from primII (Villablanca et al. 2006).

Patterning LII neuromasts

Deposition by primII begins one to two somites after the encounter with L1 (Fig. 4A), suggesting that this transient contact may somehow affect primII. We assessed this possibility by ablating primI and examining the effect on the deposition of LII neuromasts. As shown Fig. 4B, the absence of L1 has no effect on the formation of LII neuromasts. We conclude that primI plays no role in the migration of primII, nor in the onset of LII neuromast deposition around somite 9.

LII neuromasts are deposited every two somites on average (Fig. 4A–C). One would therefore expect a LII neuromast to form a doublet with the primary neuromast L2 in about 50% of the larvae. Yet this was observed in only 12% of the cases (Fig. 4C, 18 out of 148 sides, out of which 14 were L2–LII.3 and four were L2–LII.4 doublets). These observations suggest that the presence of neuromast L2 prevents the formation of a LII neuromast at the same position. This inhibitory effect would account for the observation that LII.4 neuromasts, which are usually located posterior to L2, show a much wider distribution than more anterior LII neuromasts do (Fig. 5A). In order to evaluate a putative inhibitory effect of L2, we ablated primI and examined whether the absence of L2 has an effect on the distribution of LII neuromasts. The result (Fig. 5B, black bars) shows that the distribution of LII.4 is indeed much more regular in the absence of L2, and shifted to a more anterior position. We conclude that one mechanism constraining the juvenile pattern is an inhibitory effect of LI neuromasts on the formation of LII neuromasts.

A further confirmation of the inhibitory effect of primI-derived neuromasts on the formation of LII neuromasts was obtained by taking advantage of the precocious formation of primI-derived IC neuromasts in MO-*ngn1* embryos (Grant et al. 2005). In the presence of large numbers of precocious IC between L1 and L2, the spacing between the first two LII neuromasts is much increased (Fig. 4G), suggesting that LII neuromasts compete with precocious IC neuromasts to find a place to settle. The distance increases from 2.05 ± 0.05 somites ($N = 22$) in normal embryos to 3.12 ± 0.19 somites in morphant embryos ($N = 32$), a difference that is statistically significant ($P < 0.00003$). We assume that the abnormal spacing between LII.1 and LII.2 in MO-*ngn1* embryos is due to a continued migration of LII.2 until a vacant place is found, either because no primI-derived neuromast is present, or because one neuromast has formed but has already migrated ventrally out of reach.

Phase 2: formation of IC neuromasts

IC neuromasts are easily distinguished from LII neuromasts because they are continuous with the trail of interneuromast cells, whereas LII neuromasts push the trail in front of them as they migrate ventrally (Figs. 3A and 4A). In wild type conditions, IC neuromasts can form as early as 4 dpf (Fig. 4D), but their frequency remains very low (< 0.2 per side) until the larva reaches 4 mm. The number of IC neuromasts increases progressively over the next 2 weeks, up to 12 in a 7 mm larva (Table 1).

The early distribution of IC neuromasts is centered around somite 10–12 (Figs. 4E and 5C). At later times the distribution of IC neuromasts keeps extending to more posterior regions (Figs. 2C and 5D) until all positions are occupied in the juvenile pattern (Fig. 2D). The first IC neuromasts form two
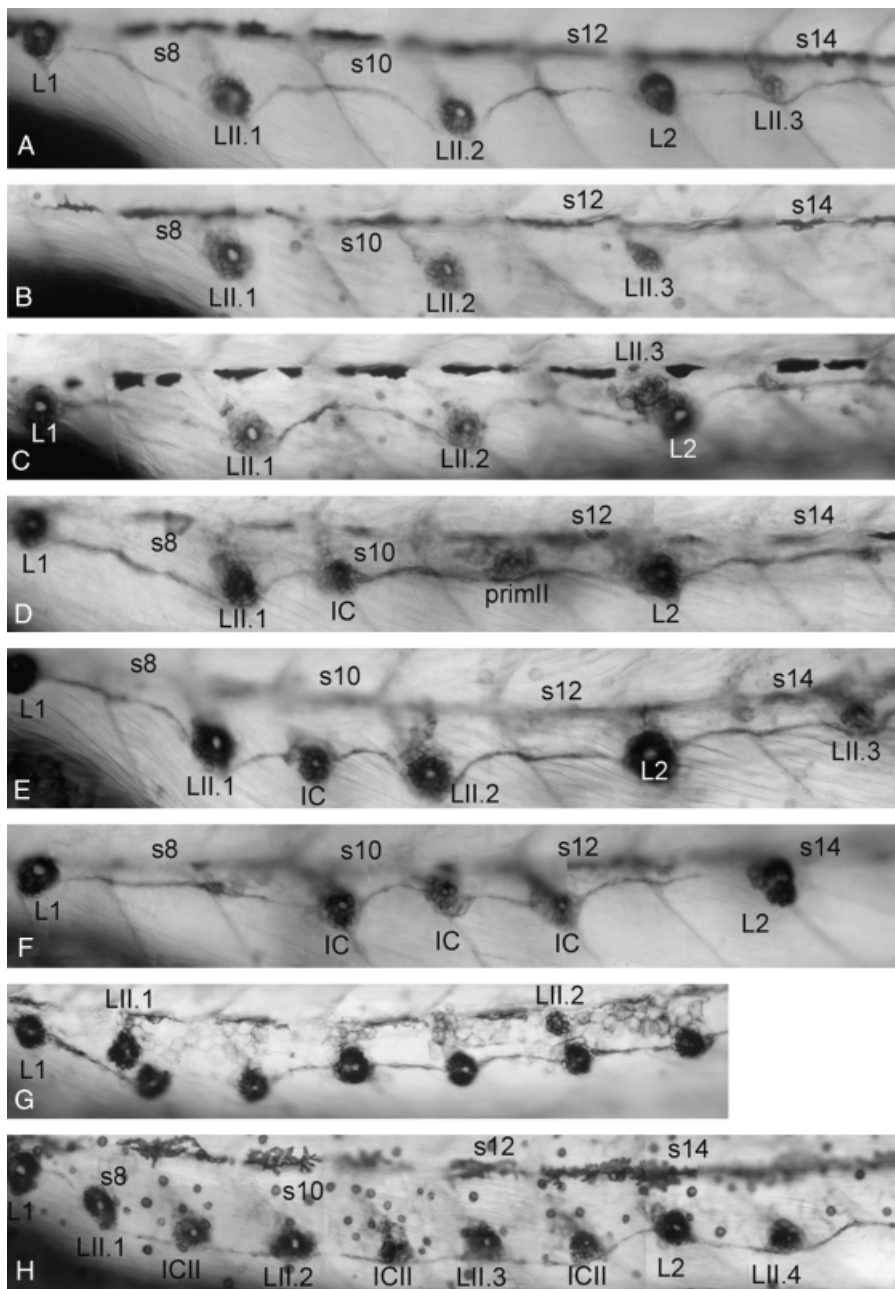
Fig. 4. Patterning of the posterior lateral line between L1 and L2. (A) Normal pattern at 5 dpf. (B) LII neuromasts in a 5 dpf larva where primI has been ablated at 24 hpf. (C) LI/LII doublet in an untreated larva. (D) IC neuromasts occasionally form prematurely (in this case, before primII has reached L2). (E) One IC neuromast is usually present in 4 mm embryos, most often on somite 10 (as was the exceptional IC of D). (F) After ablation of primII at 2 dpf, IC neuromasts form but do not show the normal bisomitic distribution. The control side of the same embryo is shown in A. (G) Abnormally large distance between LII neuromasts in a MO-*ngn1* embryo. (H) Formation of precocious primII-derived IC neuromasts after glia ablation.

somites apart, on average (Figs. 2B and 5E). IC neuromasts invariably form at positions left vacant by the LII neuromasts, and it seems likely that their bisomitic pattern reflects the bisomitic distribution of LII neuromasts. We confirmed this hypothesis by examining the distribution of IC neuromasts in the absence of LII neuromasts due to ablation of primII at 48 hpf. In this case the distribution shows no hint of a bisomitic periodicity (Figs. 4F and 5F), supporting the idea that the distribution of IC neuromasts is constrained by the presence of LII neuromasts, rather than being an intrinsic property of the interneuromast trail.

We observed that IC neuromasts are more abundant on the primII-ablated than on the control side (e.g., compare Fig. 4, F, experimental side, and A, control side of the same embryo), and that this difference is maintained throughout development (Table 2). The increase in the number of IC on the experimental side partially compensates for the loss of LII neuromasts, such that the total number of neuromasts tends to the same value on both sides of the fish. This result suggests that the competence to form IC neuromasts extends progressively from anterior to posterior during larval development, and that the total number of IC neuromasts that have formed
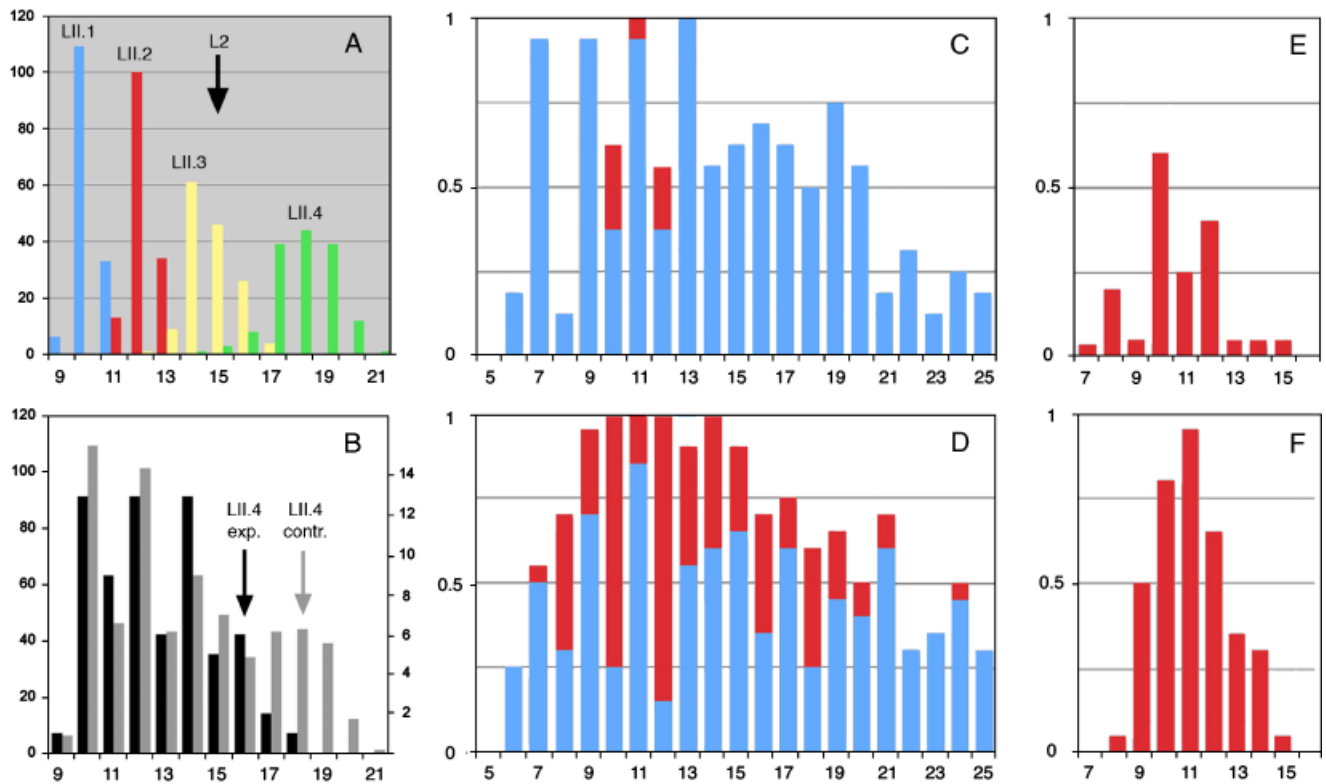
Fig. 5. Distribution of LII neuromasts and IC neuromasts. (A) Distribution of LII.1–LII.4 in wild type larvae. (B) Summed distribution of LII neuromasts in control larvae (gray bars) and in larvae where L2 is absent due to ablation of primI at 24 hpf (black bars). (C and D) Distribution of LI and LII neuromasts (blue) and of IC neuromasts (red) in 4 and 5 mm larvae, respectively. (E and F) Distribution of early IC neuromasts in control larvae (E) and in larvae where LII neuromasts are absent due to ablation of primII at 48 hpf (F). Ordinate: frequency of neuromast presence, abscissa: somitic borders.

at a given time depends on the number of sites that were preoccupied by LII neuromasts.

Phase 3a: formation of a new lateral line along the horizontal myoseptum

At 5.5 mm, the lateral (L) and the dorsal (D) lines have both migrated to more ventral positions, and have become, re-

Table 2. Formation of IC neuromasts in primII-ablated larvae

Age (dpf)	Experimental		Control		
	LII	IC	LII	IC	N
6	0	1.5	3.6	0.3	11
10	0	2.5	4.0	0.8	7
20	0	7	5.1	2.9	8
30	0	15.5	7.5	9.5	2

The data combine the results from three experiments with 7, 11, and 8 ablated embryos respectively (only embryos that completely lacked LII neuromasts on the experimental side at 5 dpf were considered).

spectively, ventral and dorso-lateral. The L′ and D′ lines then form at lateral and dorsal positions, respectively. Their completion marks the end of the larval development of the PLL (Fig. 6, A and B). The onset of the two new lines is roughly correlated with the development of the first golden stripe of iridophores of the juvenile pattern, just ventral to the horizontal myoseptum.

We noted that the neuromasts of the L′ line are oriented dorso-ventrally (Fig. 6C), as are all neuromasts derived from primII. In contrast, all neuromasts derived from primI have an antero-posterior polarity. This raised the possibility that the L′ line may be formed by primII-derived interneuromast cells. In the case of primI, interneuromast cells are readily detected between neuromasts after alkaline phosphatase labeling (Fig. 4) or in the *cldnb:gfp* line (Fig. 6D, arrowheads). They form a continuous garland of cells that is pushed ahead by primII-derived (LII) neuromasts in their ventral migration. No corresponding stripe has been described connecting LII neuromasts, however.

We examined whether primII and primD deposit interneuromast cells by using the photoconvertible marker KAEDE (Ando et al. 2002). We found that exposing the

Fig. 6. (A) Juvenile pattern in a 8 mm larva. The ventralized lateral line (L), the "new" lateral line (L′), and the ventralized dorsal line (D) are easily detected; the "new" dorsal line (D′) is too close to the dorsal midline to be seen. (B) The same fish in a more dorsal view, to show the "new" dorsal line, D′, next to the dorsal midline. Note that neither the D nor the D′ lines extend posterior to the dorsal fin. (C) Anterior neuromasts of the L and L′ lines. Note that the more dorsal (L′) neuromasts have a dorso-ventral polarity (double-headed arrows), whereas the more ventral (L) neuromasts have an antero-posterior polarity. Outline sharpening has been applied to facilitate detection of neuromast anisotropy. (D) Interneuromast cells deposited by primI and connecting the LI neuromasts to each other are readily detected in the *cldnb:gfp* line (arrowheads) as they are pushed ventrally by the migrating LII neuromasts. (E) Low-magnification view of a 48 hpf embryo where KAEDE had been photoconverted at 24 hpf in the PLL placodal region. Both primD and primII are labeled, as well as two streams of cells left behind either primordium. (F and G) Higher magnification of the interneuromast cells (arrowheads) deposited by primD and primII, respectively. The white dots outline the somitic borders in (E), primD in (F), and primII as well as the L1 neuromast, which primII is approaching in (G). Outlines were derived from Nomarski views of the same embryo. (H–J) primII-derived interneuromast cells (arrows) as revealed in SqET20 embryos, at 3 dpf (H), 4 dpf (I), and 7 dpf (J). Whereas the trail is relatively continuous at the onset (H), it quickly coalesces in discrete small clusters (J). (K) Juvenile 18 mm where primII had been ablated at 2 dpf around somite 10 on the left side. Only the two most anterior L′ stitches are present (arrows); all L′ stitches distal to the site of primII ablation are absent. (D) Control side of the same juvenile (the image has been inverted to facilitate comparison with the experimental side,K). Twelve L′ stitches extend along the flank.

region posterior to the otic vesicle to a brief pulse of UV at 24 hpf leads to a labeling of primII and primD at 48 hpf (Fig. 6E). Labeled cells extend behind primD (Fig. 6F) and behind primII (Fig. 6G), demonstrating that primII and primD leave interneuromast cells in their wake, much as primI does. The presence of putative primII-derived interneuromast cells was also noted by Grant et al. (2005) based on *eya1* expression.

primII-derived interneuromast cells are readily visualized in the ET20 line (Fig. 6, H–J, arrows). Whereas they form a continuous stripe at early times (Fig. 6H), they become dis-

continuous with time (Fig. 6J) and show large gaps in more posterior regions. The discontinuities in the distribution of primII-derived interneuromast cells may explain why the final pattern of the L′ line also comprises gaps, and is generally less regular than the final L pattern.

Contrary to their primI counterpart, primII-derived inter-neuromast cells do not move ventrally nor are they pushed ahead by later arriving neuromasts. Together with their irregular distribution, this may explain why primII-derived inter-neuromast cells are not readily detected in the *cldnb:gfp* line.

ICII neuromasts form the L′ line

Because primII deposits interneuromast cells, which remain adjacent to the horizontal myoseptum, it is conceivable that the L′ line consists of primII-derived IC neuromasts generated by these cells. We tested the possibility by ablating primII and examining whether this ablation has any effect on the formation of the L′ line. Given that the L′ line forms late, we wanted to make sure that any defect was not simply reflecting a developmental delay, and therefore we waited until the experimental fish had formed extensive stitches at every neuro-mast position. The result of the experiment is shown Fig. 6K, in a case where primII was ablated at 48 hpf at the level of somite 8, and neuromasts were revealed by DiAsp staining in a 18 mm fish. Two L′ stitches are present anterior to somite 8 in the experimental side (arrows; Fig. 6K), whereas 12 L′ stitches are present on the control side (arrows, Fig. 6L). Identical results were obtained when neuromasts were visualized by alkaline phosphatase labeling, or were revealed by GFP expression in the *cldnb:gfp* line (not shown). We conclude that the formation of the L′ line at a given antero-posterior level strictly depends on the previous migration of primII through this level.

Given the overall similarity between the formation of IC neuromasts by primI-derived interneuromast cells, and of L′ neuromasts by primII-derived cells, we wondered whether the latter are also forced into quiescence by glial cells. We used the *foxd3:gfp* line to ablate the glial cells over six somites posterior to the migrating primII. We performed the ablation at 3 dpf, when primII is usually reaching somite 9. We also ablated the ganglion on the same side, to avoid the incoming of new glial cells along regenerated axons. Ablation of the ganglion at this age has no effect on the development of IC neuromasts (not shown). We examined the pattern of LII neuromasts 5 days later (Table 3). The ablation resulted in the formation of about 2.5 additional primII-derived neuromasts on the experimental side. A clear case is shown Fig. 4H, where six consecutive LII neuromasts are observed between L1 and L2, three of which are precocious ICII neuromasts. This result supports the idea that interneuromast cells deposited by primII also require the presence of glial cells to be forced into quiescence. A few primI-derived IC neuromasts were also

Table 3. Formation of precocious ICII neuromasts after glial ablation at 3 dpf

	Experimental	Control
LI	5.2 ± 0.6	5.1 ± 0.3
LII	4.9 ± 0.9	5.2 ± 0.6
IC	1.9 ± 0.5	0.3 ± 0.6
ICII	2.6 ± 1.0	0

Glial cells were ablated in the L1–L2 interval posterior to (ahead of) primII in *foxd3:gfp* larvae. The PLL ganglion was ablated on the same side to prevent axonal regeneration and migration of new glial cells along the regenerated axons. The larvae were fixed at 9 dpf, screened for absence of GFP on the experimental side, and neuromasts were revealed by alkaline phosphatase labeling. Because it was sometimes difficult to decide whether a primII-derived neuromast was LII or ICII, we also scored the data without discriminating between LII and ICII neuromasts. The combined values were 7.5 ± 1.3 for the experimental side and 5.2 ± 0.6 for the control side, that is, 2.3 additional primII-derived neuromasts on the experimental versus the control side. Sample size: $N = 12$.

observed (Table 3), suggesting that primI-derived interneuro-mast cells may require up to 2 days of contact with glia to become stably quiescent.

Phase 3b: formation of a new dorsal line along the dorsal midline

The formation of the dorsal line by primD has not been studied so far. After migrating dorsally, primD follows a path adjacent to the dorsal midline and deposits five to six neuro-masts every two somites on average (Fig. 7A). The very dorsal location of primD makes it difficult to detect under Nomarski optics, and we have extensively relied on the *cldnb:gfp* line to visualize it properly. primD is similar to primII in size and speed of migration, but it stops migrating as it reaches the dorsal fin and lays there immobile for many days (Fig. 7A and B). D neuromasts slowly migrate ventrally, beginning with the more anterior ones, and move away from the nerve, which stays close to the dorsal midline (Fig. 7B). At this stage the primordium remains adjacent to the dorsal fin.

In the juvenile, the D line has migrated ventrally almost half way from the dorsal midline to the horizontal myosep-tum, and primD has fragmented into three to four neuro-masts that stay under the dorsal fin (Fig. 7C). We distinguish the latter neuromasts from the D1–D5 set for three reasons: first, they form much later than the other neuromasts of the D line (Table 1); second, they do not migrate ventrally, contrary to the D neuromasts, and third, they are polarized along the antero-posterior axis, contrary to all D and D′ neuromasts. Thus we call these neuromasts "terD," much as we called "ter" the terminal neuromasts of the L line.

Shortly before primD forms the terD neuromasts, the first D′ neuromasts appear close to the dorsal midline (Fig. 7B). The D′ line eventually counts five to six neuromasts. We
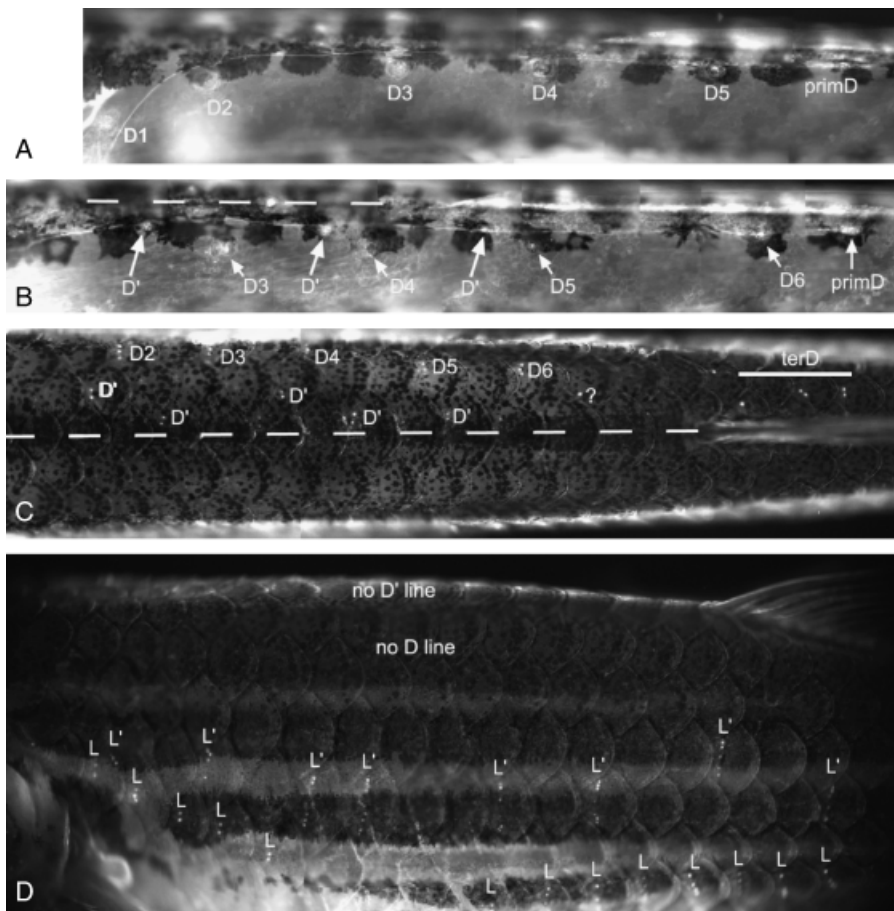
Fig. 7. Formation of the dorsal lines. (A) D line shortly after completion; primD lies immobilized under the dorsal fin. (B) After neuromasts of the D line have migrated away from the dorsal midline a new line of neuromasts, D′, is forming adjacent to the dorsal nerve. primD remains lying at the base of the dorsal fin. (C and D): Dorsal and lateral view of a 17 mm juvenile where primD had been ablated on the left side around 54 hpf, before reaching the dorsal midline. Both D and D′ lines are absent on the experimental side. The immobilized primordium has fragmented and given rise to three terD neuromasts (each of which has turned into a stitch) in the control side, but not in the experimental side.

speculated that, much like in the case of primII, primD-derived interneuromast cells might remain located along the nerve, close to the dorsal midline, and that the D′ line could be made of IC neuromasts generated by primD-derived interneuromast cells. We tested this possibility by ablating primD in the *cldnb:gfp* line at 54 hpf. We examined the effect of this ablation in fish that were 2 months old and had reached sizes of 15–20 mm. As shown Fig. 7C (dorsal view) and D (lateral view), this treatment abolishes the D line, as expected, and also the D′ line, supporting the idea that the D′ neuromasts are derived from primD. In three cases we also ablated primD after it had deposited neuromast D2 along the dorsal midline, and we observed that only the anterior most D and D′ neuromasts were present (not shown). We conclude that the new dorsal line, D′, extends precisely to the place where primD was ablated, consistent with the idea that the D′ line originates from primD-derived interneuromast cells.

DISCUSSION

We will discuss separately the three major mechanisms that contribute to the formation of the juvenile PLL pattern in

zebrafish: (1) inhibition of neuromast formation by pre-existing neuromasts, (2) formation of primI-derived IC neuromasts, (3) formation of primII/D-derived IC neuromasts (Fig. 8). We also discuss the possible implication of these mechanisms in the generation of diversity among PLL patterns of adult teleosts.

Inhibition of neuromast formation by pre-existing neuromasts

We have shown that the patterning of LII neuromasts is constrained by the presence of LI neuromasts, such that doublets comprising one LI and one LII neuromast at the same somitic border are much less frequent than chance would predict. Furthermore the few doublets that were found most often implicate L2 and LII.3. One possible explanation for this observation is that L2 is the first neuromast to undergo a ventral displacement, such that it has already left the vicinity of the horizontal myoseptum at the time primII reaches the corresponding level (about 5 dpf). This explanation implies that the inhibitory effect is either through direct contact, or through a very short-range interaction. Our observation that the distance between LII neuromasts is vastly increased in MO-*ngn1* embryos is consistent with this explanation, as most
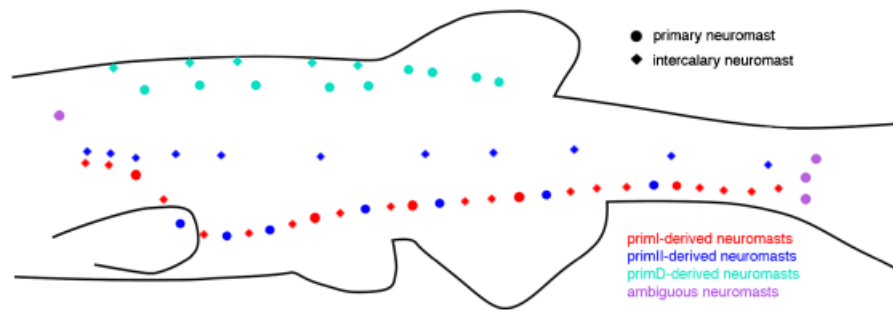
Fig. 8. Diagram of the juvenile PLL pattern illustrating the origin of each neuromast (primI in red, primII in blue or primD in turquoise) and its mode of formation (primary, i.e., deposited by a migrating primordium, or intercalary, i.e., formed through the proliferation of interneuromast cells). The neuromasts drawn in purple are derived from primI, but they are linked to the development of the primII- and primD-derived lines in the case of D1, and of the caudal lines in the case of the terminal (ter) neuromasts. The neuromasts of the anterior and caudal lateral line systems are not represented.

positions are occupied by primI-derived IC in this case, and primII would have to migrate longer before it finds a position where the IC neuromast has already migrated far enough to loose its inhibitory effect.

We also observed that IC neuromasts form and differentiate only at positions that are not already occupied by LII neuromasts. This is particularly striking in the formation of the earliest IC, which systematically appear at vacant positions, that is, at positions where neither LI nor LII neuromasts are present. This exclusion principle confers a marked bisomitic distribution to the IC pattern, complementary to the bisomitic distribution of the early LII neuromasts. We conclude that any existing neuromast inhibits the formation of another neuromast nearby through direct contact or very short-range interactions, irrespective of its own origin (primI, primII, or IC).

Formation of IC neuromasts

primI-derived interneuromast cells are made quiescent by the glial cells that accompany the PLL afferent axons, and deposition in the absence of glial cells leads to the formation of precocious IC neuromasts (Grant et al. 2005; Lopez-Schier and Hudspeth 2005). In the case of primII-derived interneuromast cells, deposition in the absence of glia also leads to the formation of precocious ICII neuromasts. We believe, therefore, that the establishment of quiescence obeys a similar mechanism for primI- and primII-derived interneuromast cells.

During normal development, interneuromast cells are relieved from quiescence and form IC neuromasts in an antero-posterior sequence. This antero-posterior progression is reminiscent of other aspects of larval maturation, such as the development of pigmented stripes, which progresses from anterior to posterior over the course of several days. It may be, therefore, that the progressive activation of interneuromast cells into IC neuromasts reflects a maturation process that spreads progressively from head to tail. This explanation

would be consistent with the observation that more IC are present when LII neuromasts are removed: if the formation of new IC takes place up to a certain A/P level at a given developmental age, then the actual number of IC will depend on how many positions are available up to this level. If fewer of these positions are already occupied, due to removal of LII neuromasts, a compensatory larger number of IC may then form on the experimental side. The relative increase in IC neuromasts on LII-depleted sides versus control sides should be observed at all ages, and this is indeed what we found.

An alternative explanation for the progressive maturation of interneuromast cells relies on their progressive deposition by primI. The time difference between deposition of interneuromast cells in the L1–L2 and in the L4–L5 intervals amounts to only 10 h, however, yet the time difference between formation of IC neuromasts in the same two intervals is more than a week. Thus minute differences in deposition times of interneuromast cells would need to be enormously amplified to account for the delayed maturation of the corresponding IC neuromasts. A nice way to evaluate this explanation would be to remove the primordium from a 24 hpf embryo and graft it, after 180° rotation, on the caudal myoseptum. If maturation depends on deposition time, one would then expect to find IC neuromasts forming from posterior to anterior. This experiment would be feasible in amphibians, through the formation of parabiotic twins (Harrison 1904), but appears technically difficult in zebrafish.

Formation of neuromasts by primII and primD

Both LII and D neuromasts are deposited every two somites on average (Fig. 4A). This pattern differs markedly from that of LI neuromasts, which have an average spacing of five somites (seven between L1 and L2, Gompel et al. 2001). A simple explanation for this difference in spacing is the vast difference in migration speed between primI on one side, and primII/primD on the other. Whereas primI travels over the trunk and tail in <24 h, primII and primD take days to reach

the level of the anus, which marks the transition between trunk and tail. The process that leads to neuromast deposition is intrinsic to the primordium (Gompel et al. 2001; Itoh and Chitnis 2001), and has recently been shown to depend on FGF signaling to initiate the formation of rosettes that prefigure the future neuromasts (Lecaudey et al. 2008; Nechiporuk and Raible 2008). Assuming this process of self-organization takes a finite amount of time to repattern the primordium after each deposition, then the distance between neuromasts will be proportional to the velocity of the primordium, that is, much greater for primI-derived than for primII- or primD-derived neuromasts.

primII and primD also deposit a stream of interneuromast cells, much as primI does, and these cells are also forced into quiescence by glial cells. Contrary to the cells deposited by primI, however, primII/D-derived interneuromast cells move very little, and remain in close vicinity to the horizontal myoseptum and dorsal midline, respectively. This explains why, when the corresponding IC neuromasts eventually form, they appear near the paths of migration of primII and primD, and form two new lines: L′ line laterally and D′ dorsally.

Oddities: D1 and terD

There are two aspects to PLL development that we need to discuss separately, even though they are unlikely to be of general relevance: the nature of the D1 neuromast, and that of terD neuromasts. D1 differs from other D neuromasts in that it is antero-posteriorly polarized, and in that its mantle cells are continuous with the primI-derived trail of interneuromast cells. Both features should lead us to include it among the primI-derived neuromasts. On the other hand, D1 forms hours after the LI line is complete, and migrates dorsally later in development, suggesting that it belongs to the D line.

D1 differentiates at around 44 hpf from a large group of cells that settle for several hours at the anterior edge of somite 1, around 34 hpf (Sapède et al. 2002). This group of cells was called D0 because video-time lapse and uncaging experiments revealed that the group splits around 34–36 hpf to form D1, primD, and primII (Sapède et al. 2002 and unpublished observations). One possible explanation for the dual nature of D1 is that the D0 cluster of cells is indeed left behind by primI as the latter begins to migrate, and is therefore part of the LI line. The D0 cluster later forms D1 but also generates primII and primD, thereby associating D1 with the dorsal line.

The case of D1 appears similar to that of the ter neuromasts, which form new primordia that colonize the caudal fin to establish the four lines of the CLL system (Dufourcq et al. 2006; Wada et al. 2008). It may be, therefore, that D1 is a link between the primI and primII/D systems, much as the ter neuromasts are the link between the PLL and CLL systems. Late events in the formation of the lateral line system may thereby be traced back to the formation of the PLL placode around 18 hpf. Interestingly, the CLL neuromasts themselves are capable of forming new primordia that generate new neuromasts upon amputation of the caudal fin (Dufourcq et al. 2006). The capability of PLL neuromasts to form new primordia after amputation has also been documented in the case of amphibians (Stone 1937).

Diversity of PLL patterns among teleosts

We have shown that a small number of mechanisms transform the embryonic to the juvenile pattern. Some of them act during embryogenesis to shape the 2 dpf pattern, and are active during larval development as well: posterior migration of the primordium and ventral migration of differentiated neuromasts. Others are observed only during postembryonic development: inhibitory effect of neuromasts on the formation of a second one at the same position, and formation of IC neuromasts from interneuromast cells. Differential control of these few mechanisms accounts for the formation of the complex, reproducible, two-dimensional (2D) juvenile pattern. Unfortunately, with the exception of the migration of primI, for which there is now considerable evidence, we do not know the molecular bases of these mechanisms.

The adult patterns of the lateral line system present very large variations among teleosts. On the contrary, the embryonic pattern is remarkably constant for all teleost species examined so far, suggesting the existence of a phylotypic stage for the teleost PLL (Pichon and Ghysen 2004). For example, the embryonic pattern in the highly derived, pelagic embryo of the tunafish *Thunnus thynnus* comprises six lateral neuromasts, the first of which has migrated dorsally, and a ter neuromast situated ventral to the horizontal myoseptum, a pattern nearly identical to that in the zebrafish (Kawamura et al. 2003, and A. Ghysen, unpublished observations). The large differences between adult teleost patterns must therefore arise mostly during postembryonic development. This raises the question of whether the mechanisms that we have identified in the zebrafish are of general relevance to all teleosts, or whether a large number of alternative mechanisms are used in different species. Analysis of postembryonic development in other species will of course be necessary to answer this question. We note, however, that the differential control of the few mechanisms at work during larval PLL development in zebrafish (antero-posterior migration of the primordia, dorsoventral migration of neuromasts, and control of neuromast density through maturation of interneuromast cells) can potentially generate an almost infinite diversity of 2D patterns.

Wada et al. (2008) have recently examined the development of neuromasts on the caudal fin of adult medaka and zebrafish. They observed that the large differences between the two patterns can be accounted for by a small number of developmental changes. They further looked at a number of other species displaying various patterns of caudal neuro-

masts and noted that dramatic differences between species can sometimes be accounted for by changes in a single process (such as, e.g., the capability of differentiated neuromasts to migrate across epidermis). They also noted that patterns that are representative of one species can sometimes be found as rare variants in another species, which normally develops a markedly different pattern, suggesting that minor differences in the control of shared mechanisms can indeed lead to major differences in PLL pattern. It seems reasonable, therefore, to imagine that most of the mechanisms that we identified in the zebrafish are also involved in shaping the postembryonic development in other species, and that the generation of diverse types of PLL patterns depends on how these few mechanisms are used and combined in individual species.

Our work has revealed the importance of time as a controlling factor that determines the PLL pattern, in addition to guidance cues. The speed of migration determines the spacing between the embryonic neuromasts, as supported by the closer spacing of primI-derived neuromasts in the *cldnb:gfp* line, where primordium migration is slowed down. The time when interneuromast cells form IC neuromasts determines the density of the pattern throughout larval life. The time when neuromasts begin to migrate through the epidermis, and their speed, may profoundly affect the final shape of each line. Because these various processes may respond differently to environmental parameters such as temperature, the development of the adult PLL might be more sensitive to external factors than that of more rigidly encoded sensory systems such as the eye. Whether this developmental plasticity contributes to speciation, or to ecological relevance, remains to be determined.

Acknowledgments

REFERENCES

Anderson, R. O., and Gutreuter, S. J. 1983. Length, weight, and associated structural indices. In L. A. Nielsen and D. L. Johnson (eds.). *Fisheries Techniques*. American Fisheries Society, Bethesda, pp. 283–300.

Ando, R., Hiroshi, H., Yamamoto-Hino, M., Mizuno, H., and Miyawaki, A. (2002). An optical marker based on the UV-induced green to-red photoconversion of a fluorescent protein. *Proc. Natl. Acad. Sci. USA* 99: 12651–12656.

Collazo, A., Fraser, S. A., and Mabee, P. M. 1994. A dual embryonic origin for vertebrate mechanoreceptors. *Science* 264: 426–430.

Dufourcq, P., Roussigné, M., Blader, P., Rosa, F., Peyrieras, N., and Vriz, S. 2006. Mechano-sensory organ regeneration in adults: the zebrafish lateral line as a model. *Mol. Cell. Neurosci.* 33: 180–187.

Ghysen, A., and Dambly-Chaudière, C. (2007). The lateral line microcosmos. *Genes Dev.* 21: 2118–2130.

Gilmour, D. T., Maischein, H. M., and Nüsslein-Volhard, C. 2002. Migration and function of a glial subtype in the vertebrate peripheral nervous system. *Neuron* 34: 577–588.

Gompel, N., Cubedo, N., Thisse, C., Thisse, B., Dambly-Chaudière, C., and Ghysen, A. 2001. Pattern formation in the lateral line of zebrafish. *Mech. Dev.* 105: 69–77.

Grant, K. A., Raible, D. W., and Piotrowski, T. 2005. Regulation of latent sensory hair cell precursors by glia in the zebrafish lateral line. *Neuron* 45: 69–80.

Haas, P., and Gilmour, D. 2006. Chemokine signaling mediates self-organizing tissue migration in the zebrafish lateral line. *Dev. Cell.* 10: 673–680.

Hammer, Ø., Harper, D. A. T., and Ryan, P. D. 2001. PAST: paleontological statistics software package for education and data analysis. *Palaeontologia Electronica* 4: 9pp. Available at http://palaeo-electronica.org/2001_1/past/issue1_01.htm.

Harrison, R. G. 1904. Experimentelle Untersuchungen über die Entwicklung der Sinnesorgane der Seitenlinie bei den Amphibian. *Arch. Mikrosk. Anat.* 63: 35–149.

Itoh, M., and Chitnis, A. B. 2001. Expression of proneural and neurogenic genes in the zebrafish lateral line primordium correlates with selection of hair cell fates in neuromasts. *Mech. Dev.* 102: 263–266.

Kawamura, G., Masuma, S., Tezuka, N., Koiso, M., Jinbo, T., and Namba, K. 2003. Morphogenesis of sense organs in the bluefin tuna *Thunnus orientalis*. In H. I. Browman and A. B. Skiftesvisk (eds.). *The Big Fish Bang. Proceedings of the 26th Annual Larval Fish Conference.* Institute of Marine Research, Bergen, pp. 123–135.

Kimmel, C. B., Ballard, W. W., Kimmel, S. R., Ullmann, B., and Schilling, T. F. 1995. Stages of embryonic development of the zebrafish. *Dev. Dyn.* 203: 253–310.

Lamason, R. L., et al. 2005. SLC24A5, a putative cation exchanger, affects pigmentation in zebrafish and humans. *Science* 310: 1782–1786.

Lecaudey, V., Cakan-Akdogan, G., Norton, W. H. J., and Gilmour, D. 2008. Dynamic FGF signaling couples morphogenesis and migration in the zebrafish lateral line primordium. *Development* 135: 2695–2705.

Ledent, V. 2002. Postembryonic development of the posterior lateral line in zebrafish. *Development* 129: 597–604.

Lopez-Schier, H., and Hudspeth, A. J. 2005. Supernumerary neuromasts in the posterior lateral line of zebrafish lacking peripheral glia. *Proc. Natl. Acad. Sci. USA* 102: 1496–1501.

Lopez-Schier, H., Starr, C. J., Kappler, J. A., Kollmar, R., and Hudspeth, A. J. 2004. Directional cell migration establishes the axes of planar polarity in the posterior lateral-line organ of the zebrafish. *Dev. Cell.* 7: 401–412.

Metcalfe, W. K. 1985. Sensory neuron growth cones comigrate with posterior lateral line primordium cells in zebrafish. *J. Comp. Neurol.* 238: 218–224.

Nechiporuk, A., and Raible, D. W. 2008. FGF-dependent mechanosensory organ patterning in zebrafish. *Science* 320: 1774–1777.

Parinov, S., Kondrichin, I., Korzh, V., and Emelyanov, A. 2004. Tol2 transposon-mediated enhancer trap to identify developmentally regulated zebrafish genes *in vivo. Dev. Dyn.* 231: 449–459.

Pichon, F., and Ghysen, A. 2004. Evolution of posterior lateral line development in fish and amphibians. *Evol. Dev.* 3: 187–193.

Raible, D. W., and Kruse, G. J. 2000. Organization of the lateral line system in embryonic zebrafish. *J. Comp. Neurol.* 421: 189–198.

Sapède, D., Gompel, N., Dambly-Chaudière, C., and Ghysen, A. 2002. Cell migration in the postembryonic development of the fish lateral line. *Development* 129: 605–615.

Stone, L. S. 1937. Further experimental studies of the development of lateral-line sense organs in amphibians observed in living preparations. *J. Comp. Neur.* 68: 83–115.

Villablanca, E., et al. 2006. Control of cell migration in the zebrafish lateral line: implication of the gene "tumour-associated calcium signal transducer," *tacstd*. *Dev. Dyn.* 235: 1578–1588.

Wada, H., Hamaguchi, S., and Sakaizumi, M. 2008. Development of diverse lateral line patterns on the teleost caudal fin. *Dev. Dyn.* 237: 2889–2902.

Webb, J. F. 1989. Gross morphology and evolution of the mechanoreceptive lateral-line system in teleost fishes. *Brain Behav. Evol.* 33: 205–222.

Webb, J. F., and Shirey, J. E. 2003. Postembryonic development of the cranial lateral line canals and neuromasts in zebrafish. *Dev. Dyn.* 228: 370–385.